International Journal of Computing and Digital Systems
ISSN (2210-142X)
Int. J. Com. Dig. Sys. 5, No.3 (May-2016)

http://dx.doi.org/10.12785/ijcds/050304

Hyperspectral Image Segmentation by Self Organized Learning-Based Active Contour Model

Fatema A. Albalooshi

Department of Computer Engineering, College of Information Technology, University of Bahrain, P.O. Box 32038, Sakheer - Kingdom of Bahrain

Received 8 Feb. 2016, Revised 8 Mar. 2016, Accepted 1 Apr. 2016, Published 1 May 2016

Abstract: The growing attention to the hyperspectral sensors is driven by their special ability to provide rich information about various objects in a scene like surface minerals, water, snow, vegetation, pollution, man-made objects, etc.; enabling effective object segmentation. In this paper, we present a hyperspectral image segmentation methodology that incorporates the local hyperspectral information into a learning-based active contour level-set function for an accurate object region and boundary extraction. The segmentation process is achieved by utilizing self-organized lattice Boltzmann active contour (SOLBAC) technique that is based on constructing a self-organized Local Image Fitting (LIF) level-set cost function, for accurate and fast boundary extraction. The proposed algorithm starts with feature extraction from raw hyperspectral images that leverages the principal component analysis (PCA) transformation to reduce dimensionality and select the best sets of the significant spectral bands. Then, the SOLBAC approach is applied on the optimal number of spectral bands determined by the PCA. By using the properties of the collective computational ability and energy convergence capability of the Lattice Boltzmann Method (LBM), our proposed segmentation is capable of producing faster segmentation by more than 30% when compared to the state-of-the-art segmentation methods. The LBM is adopted for faster curve evolution of the level-set function and to stop the evolution of the curve at the most optimum object region. Experiments performed on our test dataset show promising results in terms of time and quality of the segmentation when compared to other state-of-the-art learning-based active contour model approaches.

Keywords: Hyperspectral Image, Object Segmentation, principal Component Analysis, Self Organizing map, Lattice Boltzmann Method.

1. INTRODUCTION

Boundary extraction for object region segmentation is one of the most challenging tasks in image processing and computer vision areas. The complexity of large variations in the appearance of the object and the background in a typical image causes the performance degradation of existing segmentation algorithms. One of the goals of computer vision studies is to produce algorithms that segment object regions to produce accurate object boundaries that can be utilized in feature extraction and classification. Thus, the performance of segmentation is critical in most applications that immediately depend on the accuracy of segmentation like object interpretation, scene understanding, and image analysis [1-3].

The increasing attention to the hyperspectral sensors is motivated by great interests in developing techniques for object detection and segmentation applications [4-7]. The interest in hyperspectral technology has been sparked because it allows an opportunity for more detailed image analysis by providing different spectral signatures that indicate rich information about the different objects in the scene like surface minerals, water, snow, vegetation, pollution, manmade objects, etc.; which can facilitate effective object segmentation. In many applications, dimensionality reduction that can be defined as the process of reducing the number of bands of a hyperspectral image, is being utilized in order to map higher dimensional data into lower dimension while preserving the main features of the original data [8, 9]. Some popular techniques, such as Principal Component Analysis (PCA), Locally Linear Embedding (LLE), and Independent Component Analysis (ICA), may be used for efficient hyperspectral image analysis.

In recent years, different hyperspectral image segmentation techniques have been proposed in the literature. Some popular methods are Multinomial Logistic Regression (MLR), Markov Random Fields (MRF), Maximum Likelihood (ML), Support Vector Machines (SVM), Bayesian segmentation, Active Contour Model (ACM) and level-set methods [10-12]. Active contours approach introduced by Kass et al. [13], provides

E-mail: falbalooshi@uob.edu.bh

powerful segmentation for objects of various shapes and sizes, and maintains continuous closed boundaries in the resulting segmentation. Later on, the level-set function segmentation has been introduced by Osher and Sethian [14,15], providing a methodology for tracking curves, and resulting in accurate object boundaries. The level-set method implicitly represents the evolution of contours by embedding them as the zero level of a level-set function. Region based active contour method can be implicitly implemented using the level-set technique by leveraging the regional statistics of an input image, and it is now a reasonably familiar concept in the world of image segmentation [2, 16].

In this paper, we present a new hyperspectral image segmentation formulation using the SOLBAC technique [1] to integrate the local hyperspectral image information with the level-set function for accurate object region and boundary extraction. One advantage of this method is that the convergence of the optimum object boundary curve is simplified and speeded-up using the Lattice Boltzmann Method (LBM) [17] as an alternative approach for solving the Level-Set Function (LSF) [18, 19]. Thus, this paper utilizes a self-organized learning based active contour model with a lattice Boltzmann convergence criteria for fast and effective hyperspectral image segmentation.

The rest of the paper is organized as follows. Related work is presented in section 2. Section 3 describes the proposed methodology with detailed mathematical formulation. In section 4, experimental results are presented and discussed. Finally, section 5 outlines concluding remarks and future research direction in this technology.

2. RELAED WORK

A. Active Contour Segmentation with Prior Information

Constructing boundaries of objects using neural networks has been introduced in the literature. Leventon et al. [20, 21] first introduced the concept of incorporating prior shape information into the level-set evolution function. They provided a portrayal for the deformable shapes and defined a probability distribution over the variances of a set of training shapes. In their method, prior shape information and image information are utilized to estimate the Maximum a Posteriori (MAP) position that shapes the object in the image at every iteration of curve evolution. They used both global and local surface evolutions towards the MAP estimate and image gradients respectively.

Chen et al. [22] provide a variational level-set based segmentation that uses both shape and intensity prior information that are learned from a training set. They utilized an energy function that consists of shape and image energy parts. Image information is specified using regional intensity distributions to get rid of the heuristic weighting factor that balances image energy and shape energy terms. The learned intensity information is integrated into image model using a non-parametric density estimation method in order to yield segmentation for inhomogeneous objects.

Cremers et al. [23] present a segmentation method that combines the non-linear shape statistics with a Mumford-Shah based segmentation process. In their method, training silhouettes are utilized to drive the non-linear shape statistics by a method of density estimation. They implemented a probabilistic framework that is based on kernel Principal Component Analysis (PCA).

Sun et al. [24] developed a level-set method with shape prior to implement a shape-driven image segmentation. They utilize image moments to strip the shape priors of position, scale and angle information to obtain the aligned shape priors. Furthermore, they employed the Locality Preserving Projections (LPP) to map shape priors into a low dimensional subspace, in which the probability distribution is predicted by using kernel density estimation. The segmentation process is handled using an energy function with shape priors that combine the negative log-probability of shape priors with other data-driven energy items.

Magee and Leibe [25] proposed a framework for the combination of statistical prior information with level-set for object tracking. The level-set evolution is based on the maximization of a set of likelihoods on mesh values at features, which are located using a stochastic sampling process. Curve evolution is based on the interpolation of likelihood gradients using kernels centered at the features that are based on moments of color histogram.

Rousson and Paragios [26] provide an energetic form to integrate shape constraints to level-set representations. The shape prior construction is done using a variational approach that is based on a shape-to-area principle. They developed a shape-driven propagation energy function that incorporates level-set function with the prior shape information. The minimization of the energy function is done using calculus of variations and motion parameters.

Oktay et al. [27] present a level-set based segmentation method with shape priors that guide the level-set contortions so that the contour extraction process is excited by both the local image properties and the expert knowledge in the form of manual contours. Their system uses manual expert contours to produce new level-set surfaces which are corrupted into the surface from the level-set process. The prior information is incorporated into the level-sets by re-initializing these corrupted surfaces as new level-set surfaces.

Tabb et al. [28] proposed a framework for incorporating active contours with neural networks to produce and track the shape of a moving object in the visual field. The first stage of this method starts with tracing the boundary using Edge-Based snake ACM (EB-ACM). Then, a feed-forward error-back propagation neural network is used in the second phase of this method

as a classifier for the tracked boundary. The method starts with Sobel edge detection as a pre-processing stage followed by motion detection and blob removal procedures to produce the edges of moving objects in the image. In addition, this method used neural network with various input units and two output units, where one output unit is trained to identify human shapes, and the other for non-human shapes.

Abdelsamea et al. [29] demonstrated a segmentation method that utilizes Concurrent Self Organizing Map based on Chan-Vese model (CSOM-CV) to associate the pixel information extracted by a concurrent SOM with the level-set approach of the Chan-Vese (C-V) model [30] to construct an ACM segmentation technique.

Venkatesh et al. [31] presented a spatial isomorphism based self-organizing neural networks for active contour modeling. This method employs spatial isomorphism and self-organization in order to produce flexible boundaries that illustrate different shapes in the scene. Their implemented model is semi-automatic, in the sense that a user-interface is needed for initializing the process. In their method, a neural network isomorphic to an initial contour is constructed, and subjected to deformation in order to map onto the nearest salient contour in the image. The correspondence between the salient contour and the network is established by mapping the latter onto the former by using the self-organization scheme. Their method starts by computing the edge map of the test image; then, the initial contour points are set using an initialization scheme. For static images, the initialization is done using generalized Hough transform, while optical flow analysis or image differencing techniques are used for the initialization of video sequences. After that, the region of interest is chosen according to the location of the initial contour. Then, a SOM network is constructed isomorphic to the initial contour. Due to the reason that this contour model starts with edge detection, it yields a continuous set of points that makes it hard to distinguish an object when it is placed in a complex background.

B. The Lattice Boltzmann Method (LBM)

The Lattice Boltzmann Method (LBM) is a mathematical approach that is based on the Boltzmann equation, originally established for fluid systems simulation [17]. The application of LBM in boundary conditions has sparked from the fact that fluid dynamics particularly depend on the neighboring environment, which is mathematically characterized through the depiction of boundary conditions. The LBM method has been broadly used as an alternative to traditional fluid solvers because it can model the behavior of fluids in an approximated discrete form of space and time. This approach is efficient to solve complex non-linear Partial Differential Equations (PDEs) by discretizing space in grids (lattices) and discretizing time in time steps. Therefore, the physical space of an LBM consists of a set of uniformly spaced nodes in a lattice that describe the particles, and a corresponding set of discrete microscopic velocities of particles along with the particle distributions. The LBM can characterize Boltzmann particle dynamics using various lattice structures in 1D, 2D, or 3D. A D1Q3 lattice consists of a one dimensional lattice and three lattice speeds, while a D2Q9 lattice is a two dimensional lattice with nine lattice speeds, and a D3Q19 lattice is a three dimensional lattice with nineteen lattice speeds as shown in Fig. 1. Every link in the LBM lattice consists of a velocity vector e_i and a particle distribution $f_i(\vec{r}, t)$ that moves along that link, where $\vec{r}$ is the position of the cell, t is time, and i is the number of the link. The general evolution equation of LBM [32] is characterized as:

$$f_i(\vec{r} + \vec{e_i}, t + 1) = f_i(\vec{r}, t) + \frac{1}{\tau}\left[f_i^{eq}(\vec{r}, t) - f_i(\vec{r}, t)\right]. \quad (1)$$

Where τ is the relaxation time which is essential for stabilizing the LBM, and it controls the fluid's kinematic viscosity ϑ, given by:

$$\vartheta = \frac{1}{3}\left(\tau - \frac{1}{2}\right). \quad (2)$$

f_i^{eq} is a simplified local equilibrium particle distribution given by the Bhatnager, Gross, Krook (BGK) model [33] as:

$$f_i^{eq}(\rho, u) = \rho(A_i + B_i(e_i.u) + C_i(e_i.u)^2 + D_i u^2). \quad (3)$$

Where $A_i, B_i, C_i, and\ D_i$ are constant scalar coefficients that are specific to the chosen lattice geometry, ρ is mass, and ρu is the momentum. In classical LBMs, Equation (3) is facilitated by eliminating the momentum dependency [32] as:

$$f_i^{eq}(\rho, u) = A_i\rho. \quad (4)$$

Where $= \sum_i f_i$. In Equation (1), the equilibrium and the forcing terms are the key to recover a specific PDE.

In classical level-set active contours, a level-set equation is employed to describe the curve evolution leading to solve a PDE [14, 34-37]. The LBM approach became a recent trend for solving the level-set evolving function due to its capability to resolve the complex terms indirectly, producing a fast and effective alternative of the classical PDE solvers. Balla-Arabé et al. [18] illustrated a lattice Boltzmann based level-set image segmentation approach. They proposed a Signed Pressure Stopping Function (SPF) scheme that is based on the region based Chan-Vese ACM model [30]. The LBM is applied to solve the SPF and accomplish the convergence of the evolving contour with a higher speed. Their method accomplishes pleasing results but lacks the property of incorporating image information within the active contour model, thus resulting in over-segmentation in the cases where there is large intensity variations in the input image.

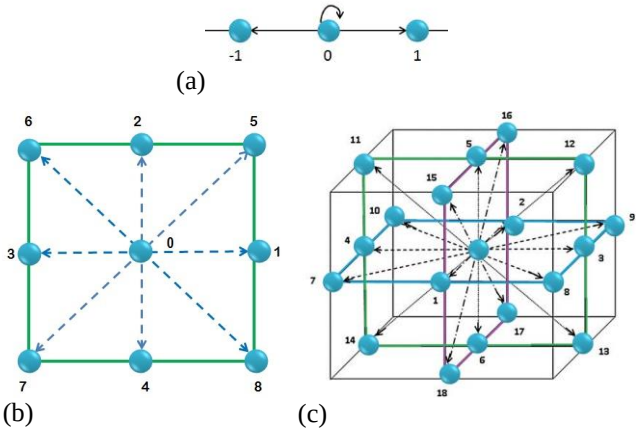

Figure 1: Illustration of lattice structure; (a) 1D structure (D1Q3); (b) 2D structure (D2Q9); (c) 3D structure (D3Q19).

3. THE PROPOSED SEGMENTATION METHOD

Our hyperspectral image segmentation methodology is based on the SOLBAC approach [1]. It starts with normalizing the row hyperspectral image in order to bring it into a computationally friendly form, then Principal Component Analysis (PCA) is utilized to reduce the dimensionality of the 240 spectral channels into 20 bands. PCA analysis shows that the resulting PCA bands are of linear combination of the original input bands. Therefore, most of the original features can be retrieved from few PCA projections [38]. We choose the first three PCA output bands to train and test our input images because information content of PCA bands decreases with an increasing number of PCA bands, thus, most of the features are constrained within the first few PCA bands [39]. Moreover, it will be more compatible with the segmentation framework. Finally, the SOLBAC approach [1] is applied for the optimum object region and boundary extraction.

A. The Self-Organizing Map

Self-organizing maps (Kohonen maps) [40], provide unsupervised spatial representations of feature vectors of input data in significantly lower dimensional output vectors known as Best Matching Units (BMUs). The BMU is determined by calculating the minimum Euclidean distance between each node's weight vector and the current input vector. Thus for an input pattern u and node's weight vector w_j, one can define BMU as:

$$BMU = \min_j \left\{ \left\| (u - w_j) \right\|^2 \right\}. \quad (5)$$

Each node in the BMU's proximity (as well as the BMU) has its weight vector modified as:

$$w_j(t+1) = w_j(t) + \Theta(t)L(t)\left\| u(t) - w_j(t) \right\|. \quad (6)$$

Where t is time step, $L(t)$ is learning rate, and $\Theta(t)$ is the amount of influence a node's distance has from the BMU on its learning. $L(t)$ is defined as:

$$L(t) = L_0 . exp\left(\frac{-t}{\lambda}\right); \quad t = 1, 2, 3, \ldots \quad (7)$$

Where L_0 is learning rate at time t_0, and $\Theta(t)$ is defined as:

$$\Theta(t) = exp\left(\frac{-\left\| (u - w_j) \right\|^2}{2\sigma(t)^2}\right); \quad t = 1, 2, 3, \ldots \quad (8)$$

Where σ is the radius of the neighborhood function. Thus, SOMs reduce dimensions and display similarities, they have been used in numerous applications such as speech and pattern recognition, meteorology, robotics, oceanography, and process control [40].

B. Learning a Level-Set Function by Self Organization

We employ a modified framework of a level-set prior-based segmentation methodology that incorporates neural networks with the level-set active contour models for accurate boundary extraction of objects in hyperspectral imagery [1]. One advantage of this method is that small seed patches from the object of interest region and other small seed patches from the background region of one single reference image are sufficiently enough to achieve the training process. The outcome of the algorithm is accurate object region boundaries. Thus, two SOM maps are employed; one SOM network to represent the object of interest, and another SOM network represents the background region. The trained networks are integrated into the next phase of the segmentation approach in which mapping of an input hyperspectral testing image is achieved. The mapped testing neurons are then exploited into the evolving curve energy function of a level-set protocol. The segmentation is accomplished by constructing a cost function that employs local image information in order to obtain the optimum boundary and region depiction of the object of interest, which holds the complete region of object of interest even if it has diverse intensity/color variations.

We utilize SOLBAC approach that employs a level-set function based on the Local Image Fitting (LIF) energy function [1, 16] defined as:

$$F^{SOM}(\phi) = \frac{1}{2}\int_{\Omega 0}^{\Omega} |I(x,y) - I^{SOM}(x,y)|^2 dxdy; x, y \in \Omega \quad (9)$$

Where Ω is the image domain, ϕ is the level-set function and I^{SOM} is the self-organizing map fitted image, defined as follows:

$$I^{SOM} = s_1 H_\varepsilon(\phi) + s_2\left(1 - H_\varepsilon(\phi)\right). \quad (10)$$

$H_\varepsilon(\phi)$ is the regularized Heaviside function given by:

$$H_\varepsilon(\phi) = \frac{1}{2}\left(1 + \frac{2}{\pi} arctan(\frac{\phi}{\varepsilon})\right). \quad (11)$$

Where ε is a positive real number that controls the width of regularization, s_1 and s_2 are the level-set foreground and background parameters, respectively, defined as:

$$s_1 = W_o - mean(I \in (\{(x,y) \in \Omega \,|\phi(x,y,t) > 0\} \cap G_k(x,y))). \quad (12)$$

$$s_2 = W_o - mean(I \in (\{(x,y) \in \Omega \,|\phi(x,y,t) < 0\} \cap G_k(x,y))). \quad (13)$$

Where W_o and W_b are the best matching neurons of the foreground object region and background region respectively, and $G_k(x, y)$ is a rectangular Gaussian window with width k.

Equation (9) is minimized with respect to ϕ to get the corresponding gradient descent flow using the lattice Boltzmann method.

C. Applying the Lattice BoltzmannMethod

According to the SOLBAC approach, the optimization of the level-set function is achieved by integrating the LIF level-set function with the LBM general equation that is defined in Equation (1), thus the improved LBM evolution equation becomes:

$$f_i((x,y) + \vec{e_i}, t+1) = F^{SOM}(x,y)\left(f_i(x,y,t) + \frac{1}{\tau}\left[f_i^{eq}(x,y,t) - f_i(x,y,t)\right] + \sigma_c\right) + F^{SOM}(x,y) f_i(x,y,t). \quad (14)$$

Where σ_c is the convection coefficient. In this paper, a D2Q5 lattice is used (Fig.2), in which, $A_i = 1/3$ for the zero central link, and $A_i = 1/6$ for the axial links.

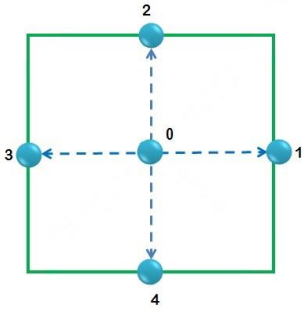

Figure 2 D2Q5 lattice structure.

Thus, a functional framework of the segmentation process is summarized in Fig.3, and the main steps for the proposed hyperspectral image segmentation are as follows:

1. Normalize the input hyperspectral image.
2. Utilize PCA for dimensionality reduction.
3. Train the object of interest SOM.
4. Train the background SOM.
5. Map the input images using the trained SOMs.
6. Apply the LIF level-set function on the mapped image.
7. Utilize LBM for fast convergence.
8. Check whether the evolution is stationary, otherwise go to step 6.

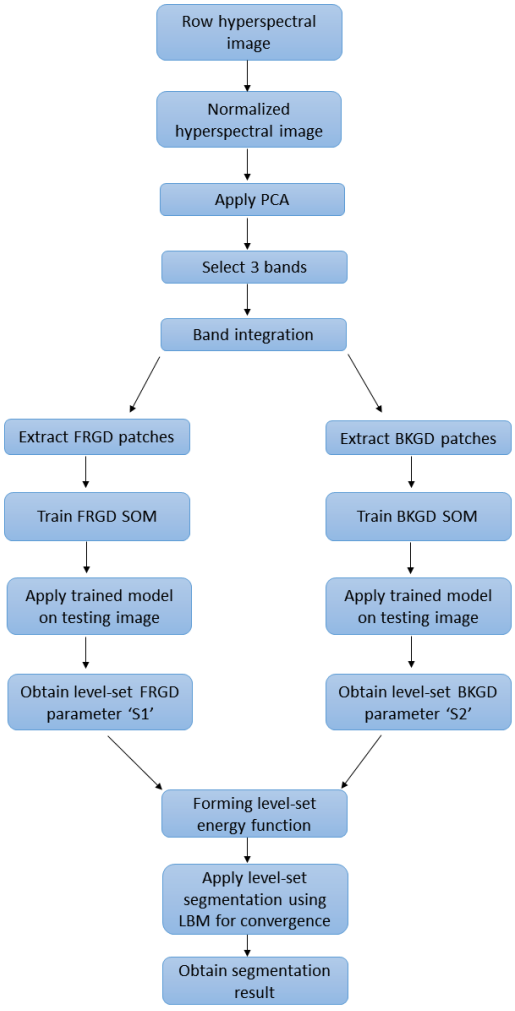

Figure 3 The functional framework of the proposed hyperspectral image segmentation system.

4. Experimental Results

To verify the effectiveness of the proposed segmentation, we use the Resonon Pika II hyperspectral camera, which provides 240 spectral channels that range from 400-900nm with 2.1nm spectral resolution, to capture real-life images and test our algorithm in various textural regions. Our experimental set consists of eight hyperspectral outdoor images, three of them were used to train our system for vegetation, cars, and vehicles, and five were used for testing. Proper evaluation of the

proposed hyperspectral image segmentation is a critical step to asses the segmentation performance; thus, in order to have fair findings, we had compared our segmentation results with other state-of-the art learning-based segmentation techniques viz. the Edge-Based Self Organizing Map ACM (EB-SOM-ACM) [28] and the Concurrent Self Organizing Map based Chen-Vese method (CSOM-CV) [29]. All experiments were conducted on a personal computer with an Intel Core I5, 2.53GHz processor, 64-bit operating system having 4.00 GB of RAM and running MATLAB R2014a.

Fig. 4(a) shows an outdoor hyperspectral image. The object of interest in this image is vegetation, therefore, the foreground SOM network is trained with a patch from vegetation and the background SOM is trained with a patch from the background (non-vegetation) region. Fig. 4(b) shows the result obtained using EB-SOM-ACM approach in which the active contours stopped at the clear gradients of the image resulting in undesirable outcome. Fig. 4(c) shows the result of the CSOM-CV method giving more accurate segmentation result illustrated by the red contours around the objects of interest. Fig. 4(d) shows the result obtained using our proposed SOLBAC approach which gives even more accurate results of the objects of interest, which is the vegetation, and excluding the windows of the background buildings. All methods introduce some false positives.

We illustrate the results of segmenting another vegetation image (trees) in Fig. 5, in which the input hyperspectral image is shown in Fig. 5(a). The SOMs were trained according to the criteria that vegetation is the object of interest and anything else to be the background region. Fig. 5(b) shows the result obtained using EB-SOM-ACM approach which provides quite good results but without obtaining complete indication of the object of interest since the output contour is not fully surrounding the vegetation area. Fig. 5(c) shows the result of the CSOMCV method giving a more accurate segmentation result illustrated by the red contours around the objects of interest. Fig. 5(d) shows the result obtained using our proposed segmentation approach giving even more accurate and precise result of the object of interest which is the vegetation, and excluding the sky in the background of the upper right corner of the image. All methods introduce some false positives.

We demonstrate the results obtained in segmenting vehicles in Fig. 6. The result obtained using the EB-SOM-ACM approach is presented in Fig. 6(b), in which the active contours stopped at the clear gradients of the image without giving good indication of the boundaries of objects of interest. Fig. 6(c) shows the result of the CSOM-CV method giving more accurate segmentation result illustrated by the red contours around the objects of interest, however, it produces some false negatives by missing a portion of the rear widow of the van and some metallic parts of the motorcycle. Fig. 6(d) shows the result obtained using our proposed segmentation approach which is quite similar to the result obtained by CSOM-CV method. All methods introduce some false positives.

The objects of interest in Fig. 7(a) are cars, therefore, the SOMs in this case were trained according to this criteria. Fig. 7(b) shows the result obtained using the EB-SOM-ACM which provides a quite good result. Fig. 7(c) shows the result of the CSOM-CV illustrated by the red contours around the objects of interest. Fig. 7(d) shows the result obtained using our proposed approach. Almost all methods produce similar results in this case and all of them introduce some false positives.

Similarly, we illustrate the results obtained in segmenting a single car in Fig. 8. The result obtained using the EB-SOM-ACM is demonstrated in Fig. 8(b). Fig. 8(c) shows the result of the CSOM-CV illustrated by the red contours around the objects of interest. Fig. 8(d) shows the outcome obtained using our proposed approach.

When comparing a segmentation method outputs to the ground truth images, there are five possible outcomes that need to be identified. The segmentation method can either (a) correctly segment a region, (b) over-segment a region, (c) under-segment a region, (d) miss a region, or (e) incorrectly segment a noise region. Therefore, it is an essential task to calculate true positives, true negatives, false positives, and false negatives - also known as confusion matrix – to evaluate segmentation performance. These are defined as follows: True Positive (TP): a pixel that belongs to the expert segmented region and was detected as "object-of-interest" by the algorithm; True Negative (TN): a pixel that does not belong to the expert segmented region and was detected as "non object-of-interest" by the algorithm; False Positive (FP): a pixel that does not belong to the expert segmented region and was detected as "object-of-interest" by the algorithm; False Negative (FN): a pixel that belongs to the expert segmented region and was detected as "non object-of-interest" by the algorithm. In addition, for evaluating segmentation methods, the following factors are also considered: Recall (RE), measures the accuracy of the system to recognize positive cases; Specificity (SP) measures the accuracy of the system to recognize negative cases; Precision(P), is the proportion of the predicted positive cases that were correct; False Positive Rate (FPR), and the False Negative Rate (FNR). An accurate segmentation system usually has high values of recall (RE) specificity (SP) and precision (P), on contrary, FPR and FNR should be small. Table 1 illustrates segmentation metrics produced after applying different learning-based segmentation techniques on our hyperspectral image dataset. The table shows better performance of our proposed hyperspectral SOLBAC segmentation approach compared to the state-of-the art approaches. Fig.9 shows a graphical representation of Table 1.

Figure 4-8 Illustration of segmentation results; (a) RGB bands of the input hyperspectral image; (b) segmentation result using EB-SOM-ACM; (c) segmentation result using CSOM-CV; (d) segmentation result using proposed approach.

Time consumption is measured for all methods. Our method performed segmentation with reduced processing time compared to processing time of the CSOM-CV and EB-SOM-ACM. Fig. 10 shows the average time consumption comparison for all methods when applied to our hyperspectral imagery dataset.

It can be observed that the proposed approach performs the segmentation process faster by more than 30% when compared to the state-of-the art learning-based segmentation methods. Because the proposed approach leverages LMB in the convergence process of the evolved contour, it can minimize the problem of time consumption. More specifically, the LBM approach is capable of solving the complex parts of the evolving curve implicitly because it discretizes space and time as described earlier in section 2, and this helps in reduction of processing time.

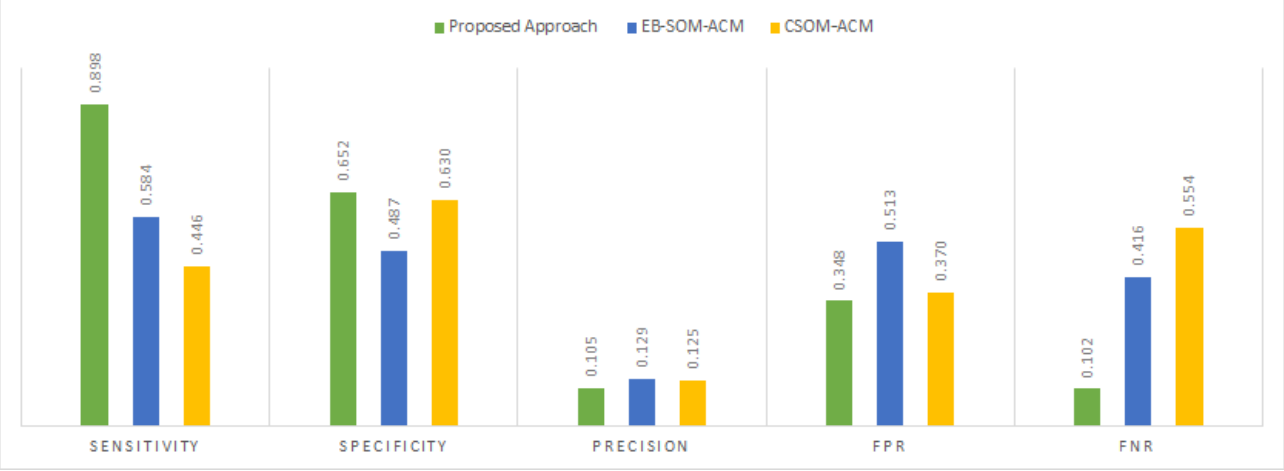

Figure 9 Graphical representation of the average segmentation statistical results.

TABLE 1 AVERAGE SEGMENTATION STATISTICAL RESULTS

Method	RE%	SP%	P%	FPR%	FNR%
Proposed approach	0.89	0.65	0.10	0.34	0.10
EB-SOM-ACM [28]	0.58	0.48	0.12	0.51	0.41
CSOM-ACM [29]	0.44	0.63	0.12	0.37	0.55

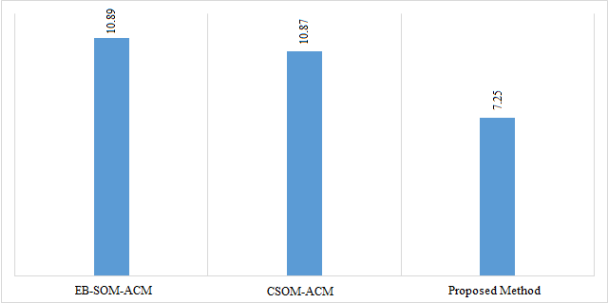

Figure 10 Average time consumption comparison for different learning-based segmentation techniques.

5. CONCLUSION

In this paper, a new fast learning-based hyperspectral image segmentation that exploits Principal Component Analysis (PCA), self-Organizing Map (SOM), Active contour Model (ACM), and Lattice Boltzmann Method (LBM) was introduced. Our method starts with PCA dimensionality reduction of raw hyperspectral imagery, then seed patches from objects of interest and other seed patches from the background were extracted to learn a dual SOMs. The learned SOMs are utilized to retrieve the prior information and integrate it in the ACM cost function in order to harvest accurate segmentation outcomes. The convergence of the ACM is achieved using LBM approach. The proposed framework was shown to effectively segment objects with lower computation time compared to other state-of-the art learning based active contour techniques. Research is in progress to employ Time Adaptive Self-Organizing Map (TASOM) for improved segmentation. In addition, the parallelization property of the LBM approach is being studied to achieve real-time segmentation.

ACKNOWLEDGMENT

The author Dr. Albalooshi acknowledges the Vision Lab research group at the University of Dayton, specifically Prof. Vijayan K. Asari and Mr. Paheding Sidike for assisting in capturing the images for testing and evaluation of the algorithm.

REFERENCES

[1] F. A. Albalooshi and V. K. Asari, "A self-organizing lattice Boltzmann active contour (SOLBAC) approach for fast and robust object region segmentation," *Image Processing (ICIP), 2015 IEEE International Conference on*, Quebec City, QC, 2015, pp. 1329-1333. doi: 10.1109/ICIP.2015.7351016

[2] Albalooshi, F.A., Asari, V.K.: Optimization of object region and boundary extraction by energy minimization for activity recognition, vol. 8750, pp. 875008-12 (2013). doi:10.1117/12.2016048. http://dx.doi.org/10.1117/12.2016048

[3] Albalooshi, F.A., Asari, V.K.: Adaptive segmentation technique for automatic object region and boundary extraction for activity recognition, vol. 8399, pp. 839907-83990711 (2012). doi:10.1117/12.919187. http://dx.doi.org/10.1117/12.919187

[4] Ball, J.E., Bruce, L.M.: Level set segmentation of remotely sensed hyperspectral images. In: Geoscience and Remote Sensing Symposium, 2005. IGARSS '05. Proceedings. 2005 IEEE International, vol. 8, pp. 5638-5642 (2005). doi:10.1109/IGARSS.2005.1526055

[5] Banerjee, A., Burlina, P., Diehl, C.: A support vector method for anomaly detection in hyperspectral imagery. Geoscience and Remote Sensing, IEEE Transactions on 44(8), 2282-2291 (2006)

[6] Alam, M.S., Sidike, P.: Trends in oil spill detection via hyperspectral imaging. In: Electrical & Computer Engineering (ICECE), 2012 7th International Conference On, pp. 858-862 (2012). IEEE

[7] Borges, J.S., Bioucas-Dias, J.M., Marçal, A.R.: Bayesian hyperspectral image segmentation with discriminative class learning. In: Pattern Recognition and Image Analysis, pp. 22-29. Springer, (2007)

[8] Kim, D.H., Finkel, L.H.: Hyperspectral image processing using locally linear embedding. In: Neural Engineering, 2003. Conference Proceedings. First International IEEE EMBS Conference On, pp. 316-319 (2003). doi:10.1109/CNE.2003.1196824

[9] Gowen, A.A., O'Donnell, C.P., Taghizadeh, M., Cullen, P.J., Frias, J.M., Downey, G.: Hyperspectral imaging combined with principal component analysis for bruise damage detection on white mushrooms [agaricus bisporus). Journal of Chemometrics 22, 259-267 (2008)

[10] Li, J., Bioucas-Dias, J.M., Plaza, A.: Spectral-spatial hyperspectral image segmentation using subspace multinomial logistic regression and markov random fields. Geoscience and Remote Sensing, IEEE Transactions on 50(3), 809-823 (2012). doi:10.1109/TGRS.2011.2162649

[11] Albalooshi, F.A., Sidike, P., Asari, V.K.: Efficient hyperspectral image segmentation using geometric active contour formulation, vol. 9244, pp. 924406-9244068 (2014). doi:10.1117/12.2067475. http://dx.doi.org/10.1117/12.2067475

[12] Borges, J.S., Bioucas-Dias, J.M., Marcal, A.R.S.: Bayesian hyperspectral image segmentation with discriminative class learning. Geoscience and Remote Sensing, IEEE Transactions on 49(6), 2151-2164 (2011). doi:10.1109/TGRS.2010.2097268

[13] Kass, M., Witkin, A., Terzopoulos, D.: Snakes: active contour models. International Journal of Computer Vision 1(4), 321-331 (1988)

[14] Osher, S., Sethian, J.A.: Fronts propagating with curvature dependent speed: Algorithms based on hamilton-jacobi formulations. Journal of Computational Physics 79(1), 12-49 (1988)

[15] Blake, A., Isard, M.: Active Shape Models. Springer, (1998)

[16] Zhang, K., Song, H., Zhang, L.: Active contours driven by local image fitting energy. Pattern recognition 43(4), 1199-1206 (2010)

[17] Succi, S.: The Lattice Boltzmann Equation for Fluid Dynamics and Beyond. Numerical mathematics and scientific computation. Oxford University Press, USA, (2001). http://www.worldcat.org/isbn/0198503989

[18] Balla-Arabé, S., Wang, B., Gao, X.: Level set region based image segmentation using lattice Boltzmann method. In: Computational Intelligence and Security (CIS), 2011 Seventh International Conference On, pp. 1159-1163 (2011)

[19] Balla-Arabé, S., Gao, X., Wang, B.: A fast and robust level set method for image segmentation using fuzzy clustering and lattice Boltzmann method. Cybernetics, IEEE Transactions on 43(3), 910-920 (2013). doi:10.1109/TSMCB.2012.2218233

[20] Leventon, M.E., Grimson, W.E.L., Faugeras, O.: Statistical shape influence in geodesic active contours. In: Computer Vision and Pattern Recognition, 2000. Proceedings. IEEE Conference On, vol. 1, pp. 316-323 (2000).

[21] Leventon, M.E., Faugeras, O., Grimson, W.E.L., Wells, W.M.: Level set based segmentation with intensity and curvature priors. In: Mathematical Methods in Biomedical Image Analysis, 2000. Proceedings. IEEE Workshop On, pp. 4-11 (2000).

[22] Chen, S., Radke, R.J.: Level set segmentation with both shape and intensity priors. In: Computer Vision, 2009 IEEE 12th International Conference On, pp. 763-770 (2009). doi:10.1109/ICCV.2009.5459290

[23] Cremers, Daniel, Timo Kohlberger, and Christoph Schnörr. "Shape statistics in kernel space for variational image segmentation." Pattern Recognition 36, no. 9 (2003): 1929-1943.

[24] Tsai, Ching-Tsorng, Yung-Nien Sun, Pau-Choo Chung, and Jiann-Shu Lee. "Endocardial boundary detection using a neural network." Pattern Recognition 26, no. 7 (1993): 1057-1068.

[25] Magee, D., Leibe, B.: On-line face tracking using a feature-driven level set. In: British Machine Vision Conference (BMVC'03) (2003)

[26] Rousson, M., Paragios, N.: Shape priors for level set representations. In: Computer Vision-ECCV 2002, pp. 78-92. Springer, (2002)

[27] Oktay, A.B., Akgul, Y.S.: Prior information based segmentation: A 3D level set surface matching approach. In: Computer and Information Sciences, 2008. ISCIS '08. 23rd International Symposium On, pp. 1-6 (2008). doi:10.1109/ISCIS.2008.4717934

[28] Tabb, K., N. Davey, R. Adams, and S. George. "The recognition and analysis of animate objects using neural networks and active contour models." Neurocomputing 43, no. 1 (2002): 145-172

[29] Abdelsamea, M.M., Gnecco, G., Gaber, M.M.: "A concurrent SOM-based Chan-Vese model for image segmentation." In: Advances in Self-Organizing Maps and Learning Vector Quantization, pp. 199-208. Springer, (2014)

[30] Chan, T., Vese, L.: "Active contours without edges". IEEE Transactions on Image Processing 10(2), 266-277 (2002)

[31] Venkatesh, Y.V., Rishikesh, N.: Self-organizing neural networks based on spatial isomorphism for active contour modeling. Pattern Recognition 33(7), 1239-1250 (2000)

[32] Zhao, Y.: Lattice Boltzmann based PDE solver on the GPU. The Visual Computer 24, 323-333 (2008). doi:10.1007/s00371-007-0191-y

[33] Bhatnagar, P.L., Gross, E.P., Krook, M.: A Model for Collision Processes in Gases. I. Small Amplitude Processes in Charged and Neutral One-Component Systems. Phys. Rev. 94, 511-525 (1954). doi:10.1103/PhysRev.94.511

[34] Peng, D., Merriman, B., Osher, S., Zhao, H., Kang, M.: A PDE-based fast local level set method. Journal of Computational Physics 155(2), 410-438 (1999)

[35] Sussman, M., Fatemi, E., Smereka, P., Osher, S.: An improved level set method for incompressible two-phase flows. Computers & Fluids 27(5), 663-680 (1998)

[36] Fedkiw, R.P., Aslam, T., Merriman, B., Osher, S.: A non-oscillatory Eulerian approach to interfaces in multimaterial flows (the ghost fluid method). Journal of Computational Physics 152(2), 457-492 (1999)

[37] Zhao, H.K., Chan, T., Merriman, B., Osher, S.: A variational level set approach to multiphase motion. Journal of computational physics 127(1), 179-195 (1996)

[38] Mather, P.M.: Computer Processing of Remotely-sensed Images: An Introduction. John Wiley & Sons, Inc., New York, NY, USA (1988)

[39] Rodarmel, C., Shan, J.: Principal component analysis for hyperspectral image classification. Surveying and Land Information Science 62(2), 115 (2002)

[40] Kohonen, T.: The self-organizing map. Proceedings of the IEEE 78(9), 1464-1480 (1990). doi:10.1109/5.58325

Fatema A. Albalooshi is an Assistant Professor at the Computer Engineering Department, University of Bahrain. She graduated from the Electrical and Computer Engineering (ECE) department of the University of Dayton in May 2015. As a graduate research assistant, Dr. Albalooshi contributed as an active member of the Computer Vision and Wide Area Surveillance Laboratory (UD Vision Lab) at the University of Dayton. Dr. Albalooshi had completed her Master of Science degree at the University of Nottingham (United Kingdom) in Electronic Communications and Computer Engineering in December 2009. Specializing in computer vision research, her primary research focus is in the field of object segmentation where she has completed more than fourteen publications in the related areas. Dr. Albalooshi's other research interests include object recognition, object tracking, image enhancement and medical imagery segmentation.